

DESIGN OF A NEUTRON DETECTOR ARRAY FOR SNM OPTIMIZED BY RADIATION TRANSPORT METHODS

Gabriel Ghita and Glenn Sjoden

Department of Nuclear and Radiological Engineering
University of Florida
202 NSB, Gainesville, FL, 32611
ghita1gm@ufl.edu

ABSTRACT

The research work presented here includes our efforts to develop a useful neutron detection device using He-3 detectors, a standard neutron detection methodology widely used in homeland security applications. The design of a He-3 neutron spectroscopy system, simulated entirely via computational methods, is proposed to resolve the spectra from Special Nuclear Materials (SNM) neutron sources of high interest. We incorporate a unique ability to effectively perform robust large-scale radiation transport simulations for SNM detection, using parallel computing methods. To demonstrate our methodology, we present the optimally detected spectral differences between SNM materials (Plutonium and Uranium), metal and oxide, using ideal filter materials. Specific focus was made to establish the limits of He-3 spectroscopy using ideal filter materials. The proposed design was then determined by replacing ideal filters with real materials, and comparing reaction rates with similar data from the ideal material suite. In our approach, we considered various configurations of moderating and attenuating materials placed around neutron sensitive detectors with a goal of isolating different parts of the neutron spectrum. To accomplish this, neutron transport simulations were performed among a suite of moderators and detectors in a “transport optimized” detector array; this enabled an optimum neutron interactions to facilitate positive detection and characterization of the incident neutrons.

Key Words: SNM, neutron detection, radiation transport, Monte Carlo, detectors

1. INTRODUCTION

The presented research work for designing a neutron detection array system for Special Nuclear Materials (SNM) neutron sources using gas proportional detectors is based on and continues our previous studies performed under the auspices of the Florida Institute of Nuclear Detection and Security (FINDS), related to the total leakage spectral characterization for a PuBe neutron source [1], SNM neutron sources [2], a Weapons Grade Plutonium (WGPu) Surrogate Source [3], and a detailed neutron energy filtering effect study [4,5].

Summarizing our preliminary work, we began by developing of a procedure for total source construction employed in the SNM computational modeling. This procedure was used throughout the research study for characterization of neutron sources. Then, using a viable computational model for the Plutonium-Beryllium (Pu-Be) neutron source capsule, we performed a complete characterization of Pu-Be leakage spectrum using deterministic [6,7] and Monte Carlo [8,9] computational techniques, and experimental validation of the model [1].

We constructed several SNM sources based on the methodology developed and validated for the Pu-Be source and performed a spectral characterization of SNM neutron sources using deterministic and Monte Carlo computational techniques. The study contains a comprehensive comparison between the metal and oxide types of neutron sources [2].

The spectral characterization of the SNM sources led us to design a shield for the Pu-Be neutron source capsule to very closely emulate a Weapons Grade Plutonium (WG Pu) metal sphere leakage neutron spectrum. This unique shield design transforms the complex neutron spectrum, through scattering, from a harder Pu-Be neutron source into a very close reproduction of a fission signature leaking from a sphere of WG Pu metal [3]. This device can be used for further laboratory experimental validation of the detection simulated models.

In support of detection assembly design, we performed a comprehensive moderator study and analyzed energy filtering effects in high density polyethylene (HDPE). In doing so, we presented a new approach utilizing four energy bands spanning the energy range; this enabled us to establish the practical limits of He-3 spectroscopy using ideal filter materials. We have demonstrated that the spectral sensitivity of neutron spectroscopy can be assessed using computational transport studies, and we finalized the moderator study with the analysis of candidate materials capable of replacing the ideal model filters [4,5].

All of this work, based on the computational radiation transport methods, enabled us to propose a design for a He-3 spectroscopy system using real filtering materials, capable of resolving the spectra from SNM neutron sources of interest (metals and oxides).

2. DETECTION DEVICE PROPOSAL

Our previous studies led us to arrive at a recommend course of action in order to isolate the four energy bands and resolve the spectra from SNM neutron sources of interest (metal and oxide).

For targeting energy Band IV, [from 31.8 keV to 369 keV], Cadmium is one of the best suitable materials. Fig.1 shows the effect on the transmitted flat neutron spectrum [4,5] through 3 cm of Cadmium (red line), together with an improved combination of 3 cm Cadmium and 1 cm Hafnium (blue line). The model of the detection assembly (block), simulated using VISED software [10] by placing the above combination of filtering materials in front of the HDPE with the rows of He-3 detectors at 2.5 cm in HDPE, is presented in Fig. 2.

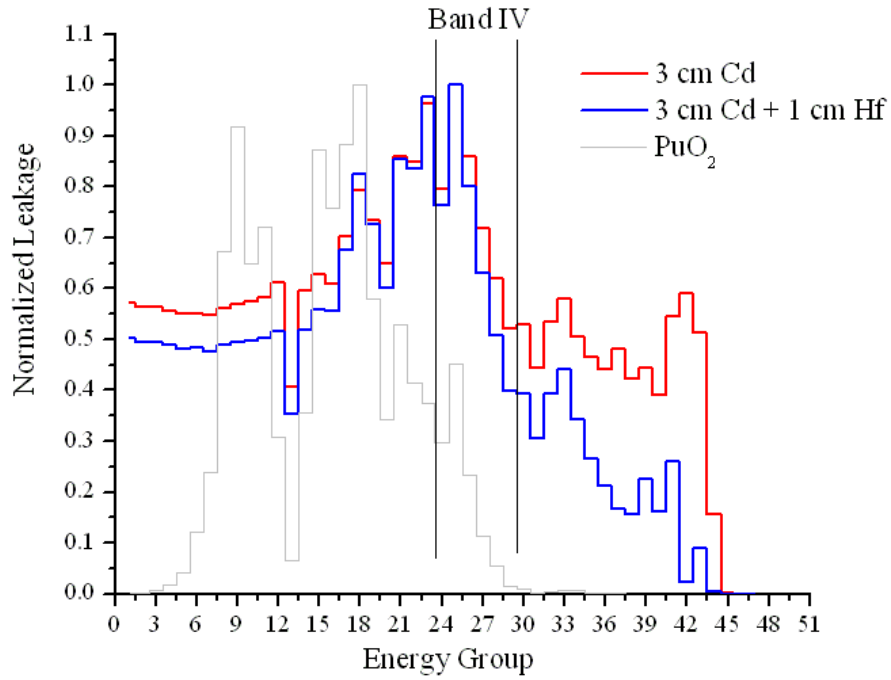


Figure 1. Targeting Energy Band IV by using 3 cm Cd and 1 cm Hf filter materials.

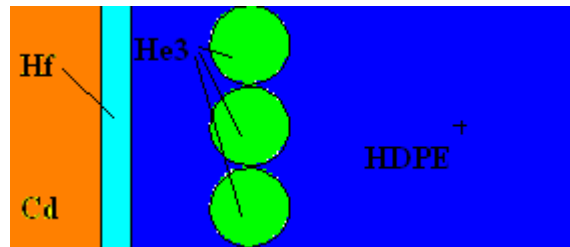


Figure 2. Block IV: 3 cm Cd, 1 cm Hf filter materials, 12 cm HDPE.

For targeting energy Band III, [from 0.369 MeV to 1 MeV], 1 cm Indium can be used as shown in Fig. 3 (red line). The blue curve in Fig. 3 illustrates that the filtering effect is improved by adding 5 mm Ta. Corresponding to the targeted energy band, the detection assembly is modeled and presented in Fig. 4 using the above combination of filtering materials in front of the HDPE with the rows of He-3 detectors at 3.0 cm in HDPE.

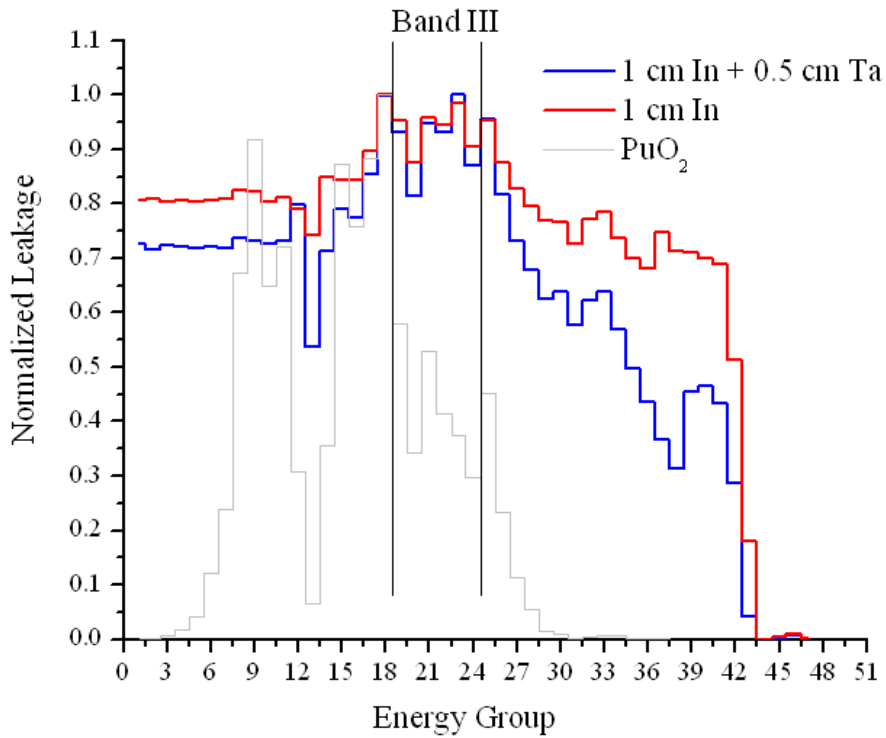


Figure 3. Targeting Energy Band III by using 1 cm In and 0.5 cm Ta filter materials.

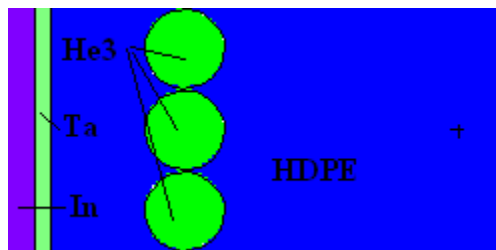


Figure 4. Block III: 1 cm In and 0.5 cm Ta filter materials, 12 cm HDPE.

For targeting energy Band II, [from 1.0 MeV to 3.68 MeV], we propose for filtering 16 cm Concrete and 1 cm Hafnium, as shown in Fig. 5. The detection block is presented in Fig. 6 where the above combination of filtering materials is placed in front of the HDPE with the rows of He-3 detectors at 3.5 cm in HDPE.

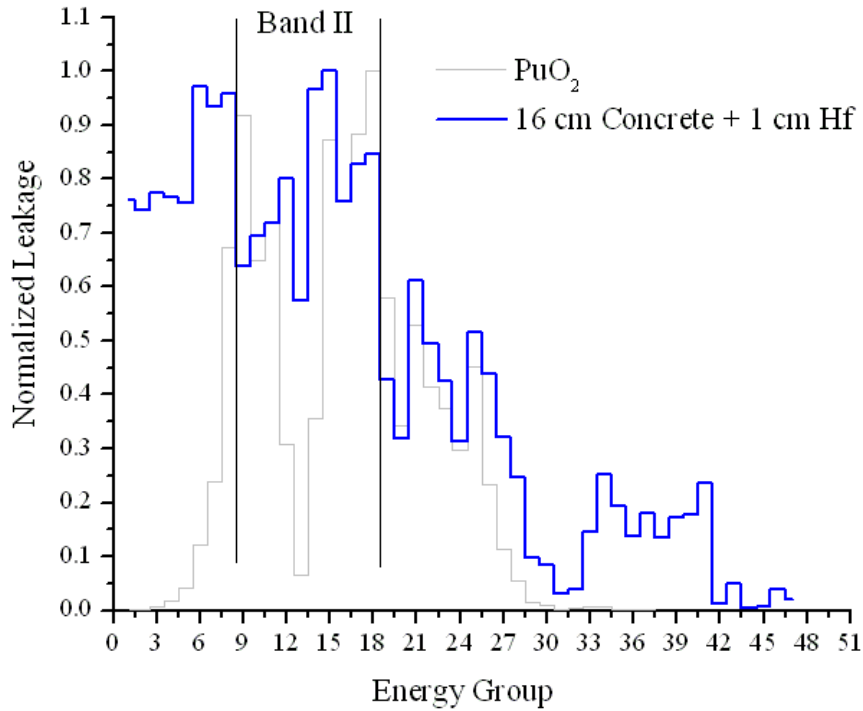


Figure 5. Targeting Energy Band II by using 16 cm Concrete and 1 cm Hf filter materials.

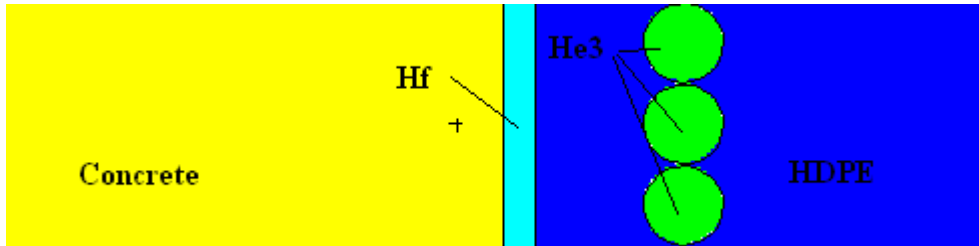


Figure 6. Block II: 16 cm Concrete, 1 cm Hf filter materials, 12 cm HDPE.

For targeting energy Band I, [from 3.68 MeV to 17.3 MeV], the best solution consists of a combination of 13 cm Asphalt and 1 mm Cadmium to remove the thermal neutrons (see Fig. 7). Corresponding to the targeted energy band, the detection block is modeled and presented in Fig. 8, by placing the above combination of filtering materials in front of the HDPE, with the rows of He-3 detectors at 4.0 cm in HDPE.

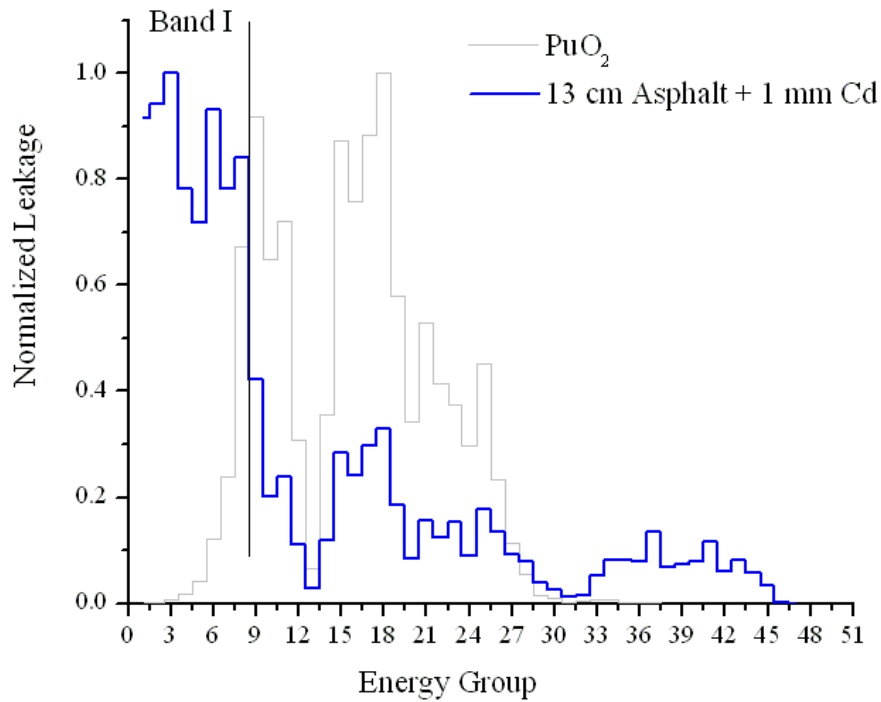


Figure 7. Targeting Energy Band I by using 13 cm Asphalt and 1 mm Cd filter materials.

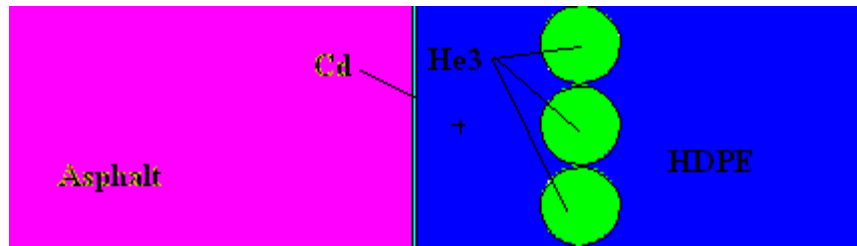


Figure 8. Block I: 13 cm Asphalt, 1 mm Cd filter materials, 12 cm HDPE moderator.

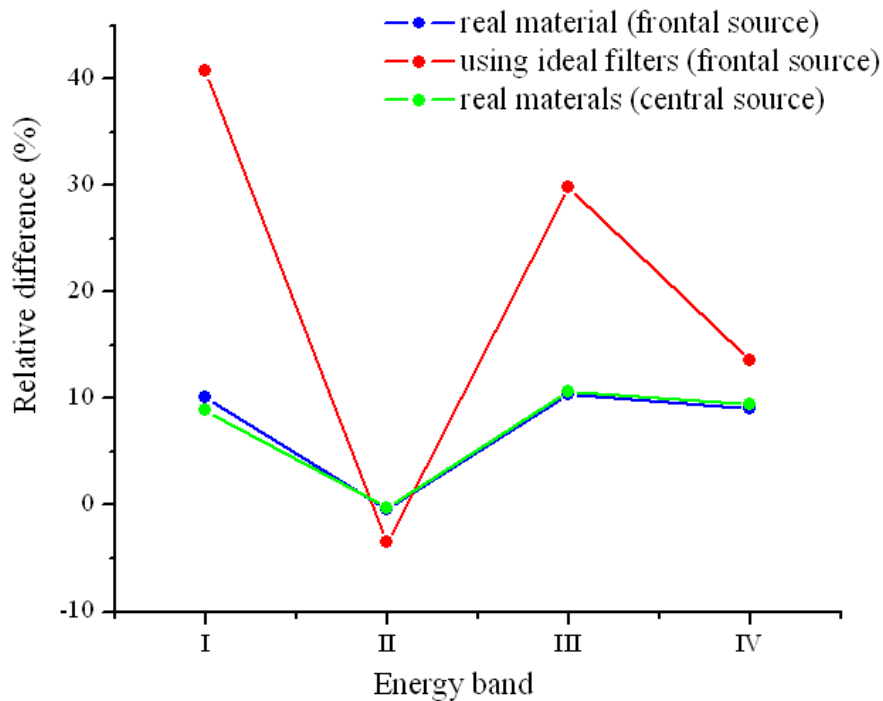
For comparison, we performed independent simulations for each detection block using the SNM neutron sources in front of the filter materials, in the same way in which we analyzed the ideal filtering case [5]. Table I (for Plutonium) and in Table II (for Uranium) present the simulated results for the detection of the neutrons corresponding to the four energy bands, together with the relative differences discernable using our approach between metals and oxides. The relevant criteria we utilized to analyze the materials selected for filtering the neutron energy bands includes the comparison between the relative reaction rate differences between metals and oxides using both ideal filters (red lines) and real materials (blue lines). These results are shown in Figures 9 (for Plutonium) and 10 (for Uranium). Due to the impracticality in removing all of the neutrons from the energy bands (other than those neutrons in the desired/measured targeted band), the features of the real material filters are smoothed compared to the ideal case results.

Table I. The reaction rate R obtained using real filter materials and Pu (frontal placed) neutron sources.

Band	Pu-metal (#/s)	1- σ	PuO ₂ (#/s)	1- σ	Rel. dif. (%)
I	14.265	0.120	12.955	0.101	10.112
II	103.320	0.506	103.730	0.498	-0.395
III	3932.000	4.325	3562.300	4.275	10.378
IV	2152.300	2.798	1973.400	2.565	9.066

Table II. The R obtained using real filter materials for U (frontal placed) neutron sources.

Band	U-metal (#/s)	1- σ	UO ₂ (#/s)	1- σ	Rel. dif. (%)
I	0.000251	0.000002	0.00816	0.00008	3147.7
II	0.002150	0.000011	0.07583	0.00038	3426.9
III	0.091790	0.000110	2.52420	0.00303	2649.9
IV	0.049320	0.000064	1.40150	0.00182	2741.5

**Figure 9. Relative difference between Pu-metal and PuO₂ generated reaction rates using ideal filtering (red line) and when employing real materials (blue line) - frontal source, and real materials (green line) - central source.**

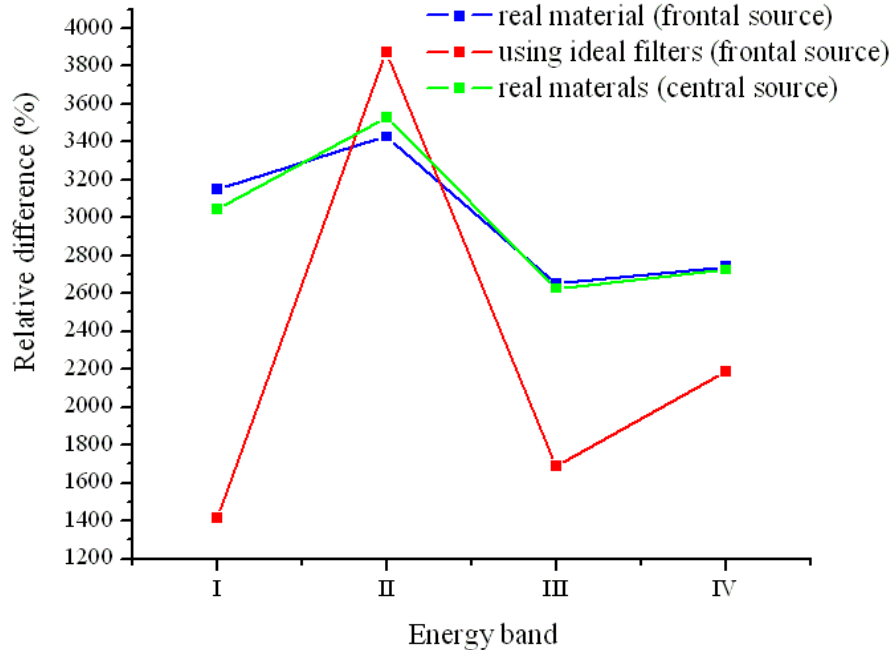


Figure 10. Relative difference between U-metal and UO₂ generated reaction rates using ideal filtering (red line) when employing real materials (blue line) - frontal source, and real materials (green line) - central source.

To prevent “cross-talk” interference, it is best to set up for the four blocks corresponding to isolation of each neutron energy band in a block material *cross*-arrangement, as shown in Fig. 11; this enables orthogonal, independent measurements of the reaction rates corresponding to the four energy bands. In Table III (Plutonium) and Table IV (Uranium) are presented the results obtained using this detection assembly with SNM neutron sources placed in the central position, 30 cm from the front faces of every detection block. In Figures 9 (for Plutonium) and 10 (for Uranium), the relative reaction rate differences between metals and oxides are depicted with a solid green line. These figures show that the differences between the results obtained via independent simulated measurements, using the SNM neutron sources directly in front of every detection block (blue line) and the results obtained by modeling the SNM sources in the center of the detection assembly (green line) are not significant.

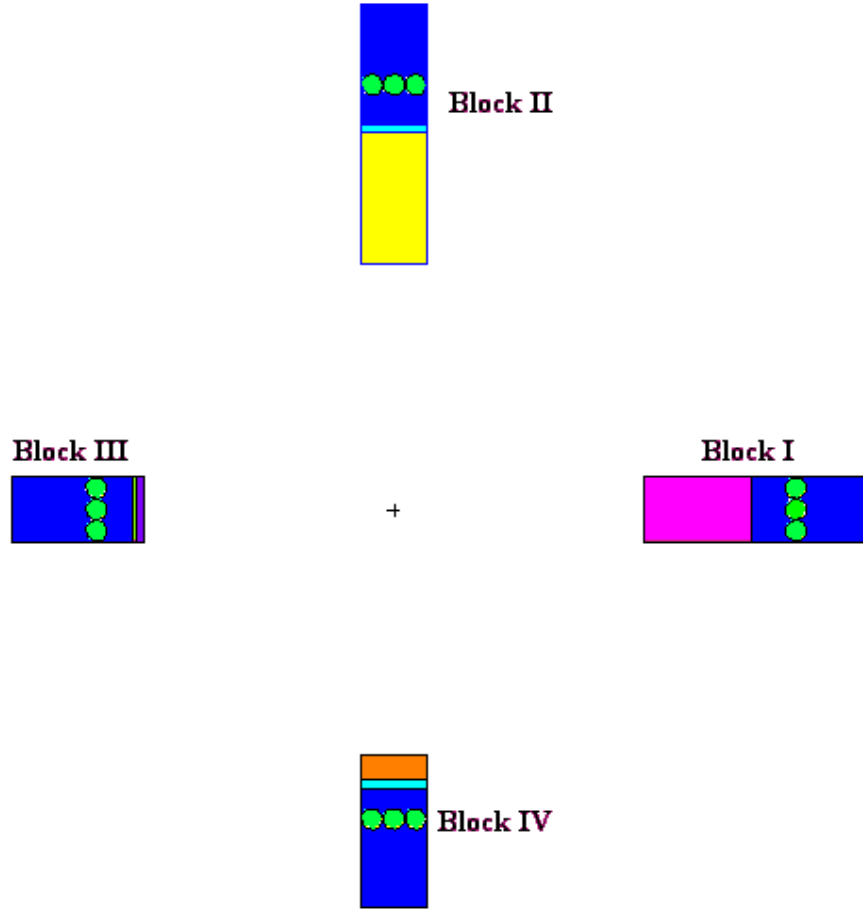


Figure 11. Detection device Assembly.

Table III. R obtained using real filter materials for Pu (central placed) neutron sources.

Band	Pu-metal (#/s)	1- σ	PuO ₂ (#/s)	1- σ	Rel. dif. (%)
I	4.002	0.018	3.676	0.017	8.861
II	13.294	0.032	13.331	0.032	-0.278
III	200.400	0.120	181.020	0.109	10.706
IV	130.100	0.104	118.810	0.095	9.503

Table IV. R obtained using real filter materials for U (centrally placed) neutron sources.

Band	U-metal (#/s)	1- σ	UO ₂ (#/s)	1- σ	Rel. dif. (%)
I	0.0000840	0.0000004	0.00264	0.00001	30.438
II	0.0002777	0.0000007	0.01008	0.00002	35.300
III	0.0047100	0.0000028	0.12839	0.00007	26.256
IV	0.0030000	0.0000024	0.08466	0.00007	27.242

Next, we can exploit the relative Ratios of the Reaction Rates from each of the four detection blocks, corresponding to the four energy bands, to directly differentiate the SNM materials; the Ratios presented in the Table V can be set up in a detection scheme electronically to yield a conclusive material “key” signature using the energy bands. We obtained a unique “fingerprint” for the SNM neutron sources, assuming that the results were not affected by background radiation (the background counts are subtracted or the system is screened against background radiation).

Table V. Relative Ratios of the R produced using SNM neutron sources*.

SNM	b3/b1	1- σ	b3/b2	1- σ	b4/b2	1- σ	b4/b1	1- σ
Pu-metal	50.081	0.250	15.074	0.045	9.786	0.031	32.513	0.169
PuO ₂	49.246	0.251	13.579	0.041	8.912	0.029	32.322	0.171
U-metal	56.085	0.297	16.960	0.054	10.803	0.037	35.723	0.196
UO ₂	48.633	0.248	12.737	0.037	8.399	0.026	32.068	0.170

*b = energy band

Two major challenges that the proposed detection device should overcome are reflected in Table V. First, consider the question related to the difficulty to differentiate between Pu-metal and oxide; there are very small differences between the reaction rate ratios obtained using the two different neutron sources. However, this impediment can be suppressed by increasing the amount of time for detection, improving the statistics of the measurements.

Analyzing the “fingerprints” of the two U neutron spectra, metal and oxide, in Table V, a much better differentiation between U-metal and oxide is possible comparing to the Pu-metal and oxide case. However, the small count rate obtainable when using U-metal neutron source (see Table IV) raises the second challenge for our proposed detection device: apart from the long time needed for measurements, background radiation can easily affect the results. Further thorough analysis is necessary to overcome these issues (e.g. performing background suppression) and to extend the practicality of the system over all neutron sources of interest.

3. CONCLUSIONS

Our analysis of the energy filtering effect in HDPE, with the new approach of four energy bands, enabled us to establish the practical limits of He-3 spectroscopy by using ideal filters. We have demonstrated that the spectral sensitivity of neutron spectroscopy can be assessed using computational transport studies and we finalized the moderator study with the analysis of candidate materials capable of replacing the ideal filters.

Corroborating our research work, we recommend a design of a neutron detector array that can resolve SNM neutron spectra from sources of interest (metal and oxide), to the greatest extent permissible, based on four energy band separation in HDPE, using He-3 detectors and specifically tailored filtering materials.

Construction and testing the proposed neutron detector assembly is a possibility for a future work. However, a careful analysis of background and skewing effects on the fingerprints of the SNM neutron sources, particularly for Uranium neutron sources, is strongly recommended. Moreover, a study of the environmental effects on the SNM detection “key” signatures for different scenarios can be another extremely useful study. Different geometry perturbations, depending on the detection scenario, may also be necessary.

ACKNOWLEDGMENTS

This project was made possible through the support of National Nuclear Security Administration (NNSA).

REFERENCES

1. G. GHITA, G. SJODEN, and J. BACIAK, “A Methodology for Experimental and 3-D Computational Radiation Transport Assessment of Pu-Be Neutron Sources”, *Nuclear Technology*, **159**, pp.319-331, (2007).
2. G. GHITA, G. SJODEN, and J. BACIAK, “Comparison of 3-D Deterministic Parallel and Monte Carlo Transport Computations for Special Nuclear Materials Assessments”, *Proceedings of PHYSOR-2006, Advances in Nuclear Analysis and Simulation*, Vancouver, BC, Canada, September 10-14, 2006.
3. G. GHITA, G. SJODEN, and J. BACIAK, “Computational and Experimental Validation of a WGPu Neutron Leakage Source Using a Shielded PuBe (α,n) Neutron Source,” accepted to *Nuclear Technology*, 2008.
4. G. GHITA, G.E. SJODEN, J. BACIAK, and N. HUANG, “3D Computational and Experimental Radiation Transport Assessments of Pu-Be Sources and Graded Moderators for Parcel Screening,” *Proceedings of SPIE, International Society for Optical Engineering, Defense and Security Symposium*, **6213**, pp.I01-I015, Orlando, Florida, April 17-21, (2006).
5. G. GHITA, G. SJODEN, and J. BACIAK, “On Neutron Spectroscopy Using Gas Proportional Detectors Optimized by Transport Theory,” submitted to *Nuclear Technology Journal*, 2008.
6. G. SJODEN and A. HAGHIGHAT, “PENTRAN - A 3-D Cartesian Parallel S_N Code with Angular, Energy, and Spatial Decomposition”, *Proceedings of the Joint International Conference on Mathematical Methods and Supercomputing for Nuclear Applications*, p. 553, Saratoga Springs, NY, October 5-10, 1997.
7. “BUGLE-96: A Revised Multi-group Cross Section Library for LWR Applications Based on ENDF/B-VI Release 3,” J. WHITE, D. INGERSOLL, C. SLATER, and R. ROUSSIN, DLC-185, Oak Ridge National Laboratory, Oak Ridge, TN, (1996).
8. “A General Monte Carlo N-Particle Transport Code, Version 5X-5”, MONTE CARLO TEAM, MCNP5 —, LA-UR-03-1987, Los Alamos National Laboratory, Los Alamos, NM, (2003).

9. "A Nuclear Cross Section Databook", H. M. FISHER, LA-11711-M, Los Alamos National Laboratory, Los Alamos, NM, (1989).
10. R. A. SCHWARZ and L. L. CARTER, "Visual Editor to Create and Display MCNP Input Files," *Transactions of the American Nuclear Society*, **77**, 223, (1997).